Supporting Information

Fast Charge Diffusion in $MAPb(I_{1-x}Br_x)_3$ Films for High-Efficiency Solar Cells Revealed by Ultrafast Time-resolved Reflectivity

Wenjun Shi[a], Yong Wang[b], Taiyang Zhang[b], Haijuan Zhang[a], Yixin Zhao[b, *], Jie Chen[a, *]

[a]*Center for Ultrafast Science and Technology, Key Laboratory for Laser Plasmas (Ministry of Education), School of Physics and Astronomy, Collaborative Innovation Center of IFSA (CICIFSA), Shanghai Jiao Tong University, Shanghai 200240, China*

[b]*School of Environmental Science and Engineering, Shanghai Jiao Tong University, Shanghai 200240, China.*

1. Sketch of the experimental setup

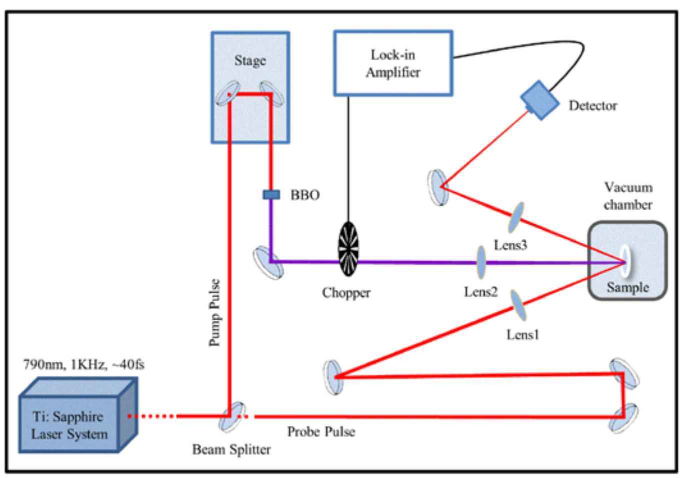

Figure S1. Experimental setup of femtosecond time-resolved reflectivity measurements.

2. Fitting for the recovery process using different functions

* Corresponding authors.
E-mail address: yixin.zhao@sjtu.edu.cn (Y. Zhao); jiec@sjtu.edu.cn (J. Chen).

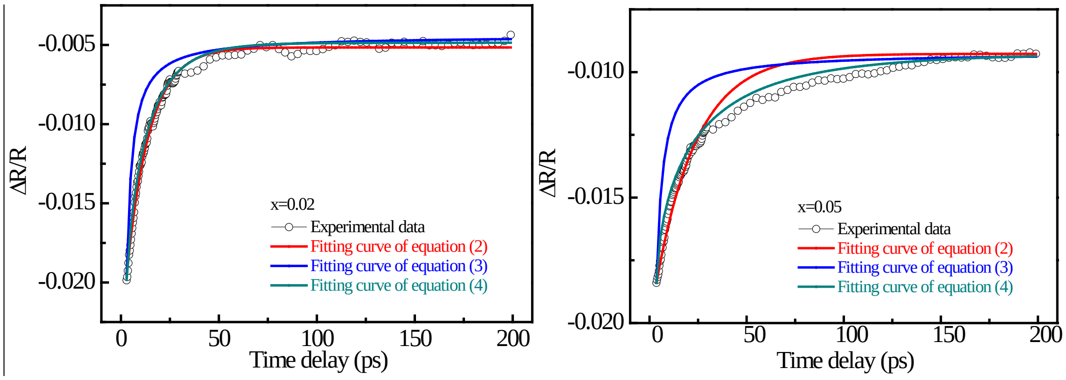

Figure S2. Comparison between the fitting effects using different functions for the decay processes of $MAPb(I_{1-x}Br_x)_3$ with x=0.02 and 0.05.

We try to fit the decay processes of $MAPb(I_{1-x}Br_x)_3$ using the following equations:

$$\frac{\Delta R}{R}(t) = \beta n_0 e^{-\frac{t-t_0}{\tau_1}} \tag{2}$$

$$\frac{\Delta R}{R}(t) = \beta \frac{n_0}{Bn_0(t-t_0)+1} \tag{3}$$

$$\frac{\Delta R}{R}(t) = \beta n_0 e^{-\left(\frac{(t-t_0)}{\tau_k}\right)^{\gamma}} \tag{4}$$

which describes the first-order charge carrier diffusion mechanism, the second-order free electron and hole recombination mechanism and the combination of these two mechanisms, respectively. Using equation (2), the decay processes for $MAPb(I_{0.99}Br_{0.01})_3$ and $MAPb(I_{0.98}Br_{0.02})_3$ can be well reproduced, while for $MAPb(I_{1-x}Br_x)_3$ films with other Br contents, the fitting curves deviate from the experimental data. Using equation (3), all the fitting curves deviate significantly from the experimental data. However, using equation (4) with a γ fluctuating between 0.50 and 0.95, all the decay processes can be well reproduced. These phenomena indicate that the photocarriers decay through a complex combination of the two competing mechanisms, neither a simple first-order nor a second-order mechanism alone.

3. Sample preparation and properties

The $MAPb(I_{1-x}Br_x)_3$ films used in this study were prepared by a spin-coating method. To fabricate $MAPb(I_{1-x}Br_x)_3$ with different Br contents, precursor solutions with different Br concentration were prepared by mixing $MAPbI_3$ and $MAPbI_2Br$ solutions in different proportions. The fabrication details have been described elsewhere [1]. In Figure S3, we present the X-ray diffraction (XRD) patterns for part $MAPb(I_{1-x}Br_x)_3$ films. The XRD peak intensities for $MAPb(I_{0.99}Br_{0.01})_3$ and $MAPb(I_{0.98}Br_{0.02})_3$ are much higher than those for other films, indicating that $MAPb(I_{0.99}Br_{0.01})_3$ and $MAPb(I_{0.98}Br_{0.02})_3$ have better grain morphologies. In Figure S4a, we show the absorption spectra of the $MAPb(I_{1-x}Br_x)_3$ films. As the Br content rises up, the absorption edge of $MAPb(I_{1-x}Br_x)_3$ shifts gradually to the blue side, which has been observed in previous reports [2-3]. In Figure S4b, we summarizes the relationship between the absorption edge (λ_e) of $MAPb(I_{1-x}Br_x)_3$ and x, which can be described using the following equation

$$\lambda_e(\mathrm{nm}) = 777.8 - 279.6\mathrm{x}. \tag{S1}$$

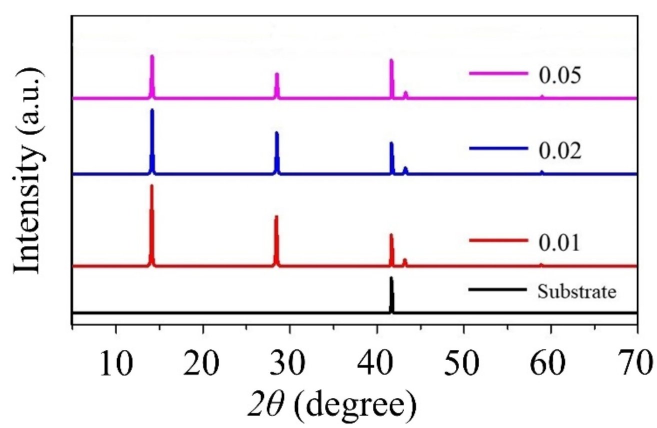

Figure S3. XRD patterns of part $MAPb(I_{1-x}Br_x)_3$ films.

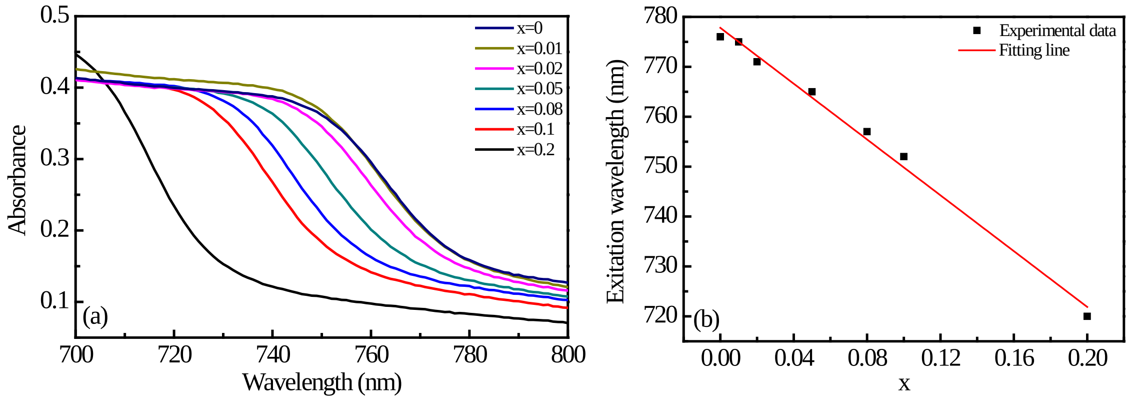

Figure S4. (a) Absorption spectra of $MAPb(I_{1-x}Br_x)_3$ with different Br contents; (b) The relationship between the absorption edge and the Br content (x) for $MAPb(I_{1-x}Br_x)_3$.

In Figure S5, we reproduce the x dependence of PCE for $MAPb(I_{1-x}Br_x)_3$ films from our previous reported data [4]. For $MAPb(I_{1-x}Br_x)_3$ with $x \approx 0.02$, the PCE is 19.12%, which is at least 8% higher than that for $MAPb(I_{1-x}Br_x)_3$ with other Br contents. In previous [4], the $MAPb(I_{1-x}Br_x)_3$ films were prepared using a two-step fabrication method, i.e. prepare the pure $MAPbI_3$ films firstly, and then treat them using MABr solutions with different concentrations. By this two-step fabrication method, the Br contents could not be obtained directly. However, the absorption edges of those $MAPb(I_{1-x}Br_x)_3$ films show a similar blue shift as $MAPb(I_{1-x}Br_x)_3$ films used in this study. Thus, the Br contents for those $MAPb(I_{1-x}Br_x)_3$ films can be estimated using equation (S1). Br contents of $MAPb(I_{1-x}Br_x)_3$ fabricated by treating the $MAPbI_3$ film using 1, 2, 4 and 8 mg ml^{-1} MABr isopropanol solutions are x=0.006, 0.019, 0.037 and 0.050, respectively.

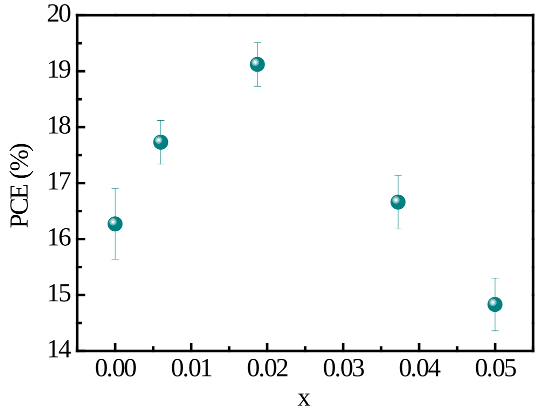

Figure S5. Br content dependence of PCE for $MAPb(I_{1-x}Br_x)_3$ films.

Reference

1. Zhao, Y.; Nardes, A. M.; Zhu, K., Mesoporous Perovskite Solar Cells: Material Composition, Charge-Carrier Dynamics, and Device Characteristics. *Faraday Discuss.* **2014,** *176*, 301-312.

2. Noh, J. H.; Im, S. H.; Heo, J. H.; Mandal, T. N.; Seok, S. I., Chemical Management for Colorful, Efficient, and Stable Inorganic-Organic Hybrid Nanostructured Solar Cells. *Nano Lett.* **2013,** *13*, 1764-1769.

3. Sadhanala, A.; Deschler, F.; Thomas, T. H.; Dutton, S. E.; Goedel, K. C.; Hanusch, F. C.; Lai, M. L.; Steiner, U.; Bein, T.; Docampo, P.; Cahen, D.; Friend, R. H., Preparation of Single-Phase Films of $CH_3NH_3Pb(I_{1-x}Br_x)_3$ with Sharp Optical Band Edges. *J. Phys. Chem. Lett.* **2014,** *5*, 2501-2505.

4. Yang, M.; Zhang, T.; Schulz, P.; Li, Z.; Li, G.; Kim, D. H.; Guo, N.; Berry, J. J.; Zhu, K.; Zhao, Y., Facile Fabrication of Large-Grain $CH_3NH_3PbI_{3-x}Br_x$ Films for High-Efficiency Solar Cells via CH_3NH_3Br-Selective Ostwald Ripening. *Nat. Commun.* **2016,** *7*, 12305-12313.